A second wave of topological phenomena in photonics and acoustics

https://doi.org/10.1038/s41586-023-06163-9

Received: 28 July 2022

Accepted: 3 May 2023

Published online: 21 June 2023

Check for updates

Xiujuan Zhang[1], Farzad Zangeneh-Nejad[2], Ze-Guo Chen[3], Ming-Hui Lu[1]✉ & Johan Christensen[4]✉

Light and sound are the most ubiquitous forms of waves, associated with a variety of phenomena and physical effects such as rainbows and echoes. Light and sound, both categorized as classical waves, have lately been brought into unexpected connections with exotic topological phases of matter. We are currently witnessing the onset of a second wave of active research into this topic. The past decade has been marked by fundamental advances comprising two-dimensional quantum Hall insulators and quantum spin and valley Hall insulators, whose topological properties are characterized using linear band topology. Here, going beyond these conventional topological systems, we focus on the latest frontiers, including non-Hermitian, nonlinear and non-Abelian topology as well as topological defects, for which the characterization of the topological features goes beyond the standard band-topology language. In addition to an overview of the current state of the art, we also survey future research directions for valuable applications.

For many years, there have been persistent efforts to find novel ways to manipulate light and sound waves, which are two important sources of energy and information with which we perceive the world. Conventional wisdom is to control the frequency, polarization, amplitude and phase, which are fundamental and intrinsic degrees of freedom widely exploited within the field of metamaterials[1,2]. Very recently, the topology degree of freedom that relies on symmetries has offered an alternative and unprecedented approach for light and sound manipulation, leading to novel photonic and acoustic topological structures beyond the realm of metamaterials. Ruled by the symmetry-protected topological order, the hallmark of topological insulators (TIs) is interfacial edge states, which are governed by the bulk–edge correspondence relating these states to bulk topological invariants[3,4]. This unusual and non-trivial design paradigm for classical waves particularly came into fruition through the ability to enable robust, defect and disorder-immune waveguiding. Moreover, long-established experimental photonic and acoustic platforms offer a versatile setting for the studies of these novel topological phases, owing to well-controlled material processing and mature characterization techniques[5–9].

Tracing the developments of topological photonics and acoustics, one first encounters the quantum Hall insulators, also known as Chern insulators. Such kinds of TIs are characterized by a quantized topological invariant, that is, the Chern number[10], which is defined by the number of monopoles associated with the Berry flux in the momentum space[5]. Manifested by chiral edge states in the bandgaps, quantum Hall insulators imply breaking of the time-reversal ($\mathcal{T}$) symmetry. For example, gyromagnetic materials subject to magnetic fields and circulating airflows violate the $\mathcal{T}$ symmetry for electromagnetic and acoustic waves, respectively, giving rise to classical analogues of the quantum Hall effect[11–16]. An alternative strategy towards this goal relies on applying a time-harmonic modulation of the involved constituents in photonic and sonic crystals. By properly adjusting the modulation, an effective magnetic field can be produced, leading to a non-trivial topology. Such kinds of topological system, dubbed Floquet TIs, have been widely investigated in both photonics[17,18] and acoustics[19,20], featuring the same gapless edge states[5] as those of unmodulated quantum Hall insulators. Other schemes to realize effective magnetic fields or equivalent fluxes have also been suggested via strains[21], chiral[22] or negative couplings[23].

On another front, topological configurations with intact $\mathcal{T}$ symmetry have emerged in the context of spin Hall insulators or $\mathbb{Z}_2$ TIs, featuring spin-dependent in-gap edge states[24–27]. The key ingredient of such TIs is the spin–orbital coupling, which has been realized in photonic and acoustic systems using different techniques. By manipulation of either the polarization or the lattice degree of freedom, and/or degenerate Bloch modes, the so-called Kramers-like degeneracies, comprising pseudospins that are protected by quantized $\mathbb{Z}_2$ topological invariants, were constructed[28–33]. Also, with preserved $\mathcal{T}$ symmetry but with either broken inversion or mirror symmetries, multifaceted geometrical photonic and acoustic designs have paved the way for valley Hall TIs using artificially engineered hexagonal lattices[34–37].

Recent developments of higher-order TIs[38] have also greatly benefited from the versatile photonic and acoustic designs, leading to novel topological systems, including dipole and multipole insulators[39–48]. These higher-order TIs host multidimensional topological states, which have also been realized in other platforms such as electric circuits[49–52]. In addition to TIs with bandgaps, gapless topological structures have attracted a lot of attention in photonics and acoustics[53]. Such structures

[1]National Laboratory of Solid State Microstructures and College of Engineering and Applied Sciences, Nanjing University, Nanjing, China. [2]Hitachi ABB Power Grids Research Center, Baden, Switzerland. [3]School of Materials Science and Intelligent Engineering, Nanjing University, Suzhou, China. [4]IMDEA Materials Institute, Madrid, Spain. ✉e-mail: luminghui@nju.edu.cn; johan.christensen@imdea.org

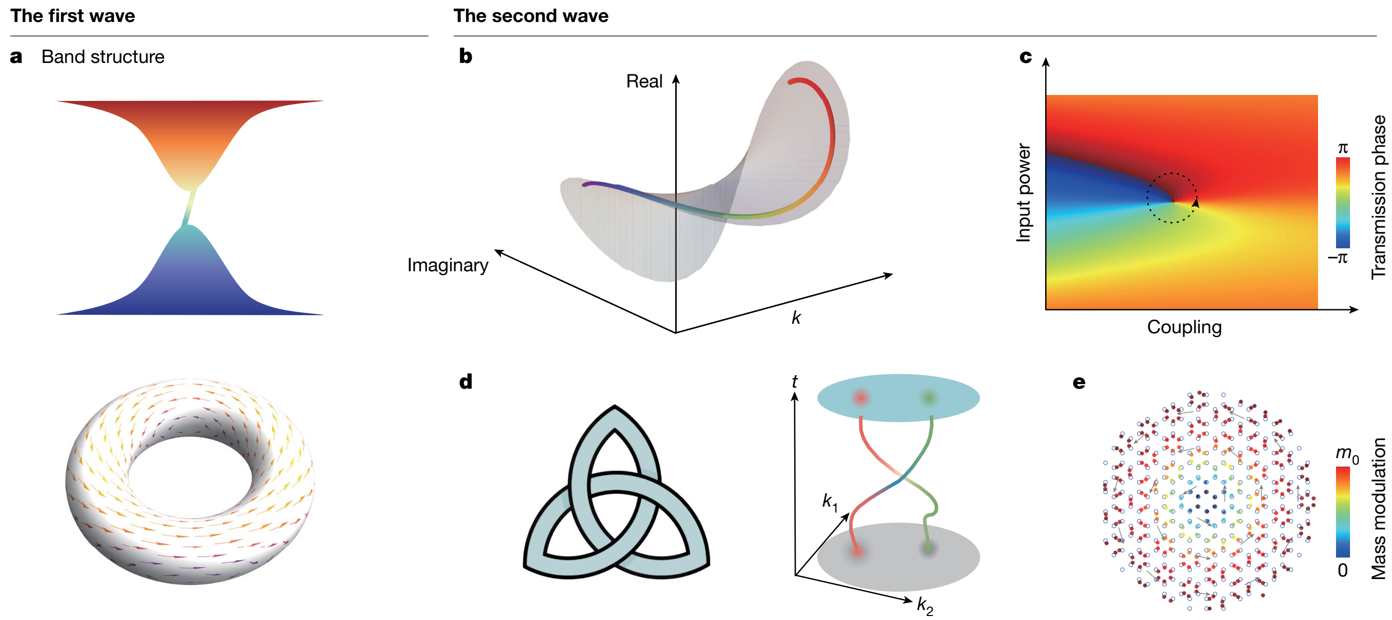

Fig. 1 | Beyond conventional topological systems. a, A typical band structure (top) and the non-trivial Berry curvature (bottom) for conventional TIs. The integral of the non-trivial Berry curvature over the Brillouin zone, which is isomorphic to a torus in two dimensions, gives rise to the topological invariant that characterizes the non-trivial topology. As a result, topological edge states emerge in the bulk bandgap as the top illustration shows. **b**, A topological non-Hermitian band characterized by complex-energy winding. Such winding is defined by the eigenenergy trajectory forming closed loops in the complex-energy plane, which is fundamentally different from the conventional TIs depicted in **a**, where the non-trivial topology is characterized by eigenstate winding. **c**, The topology of a nonlinear system is different from the linear counterpart and cannot be defined using the traditional methods, because it is not feasible to determine the band structure of a nonlinear system. However, the topological index can be identified by alternative approaches, for instance, by analysing the transmission phase and its winding behaviour as the input power to the system is increased. **d**, Compared with Abelian gap topology and the robust edge state in **a**, band-degeneracy-formed knot and braid structures in the energy dispersion are also robust against perturbations. The left panel shows the simplest non-trivial trefoil knot, whose knot group is isomorphic to the non-Abelian braid group B_3 with three strands. The right panel shows a basic braid plot with two strands. **e**, A vortex defect is shown, whose topology originates from the distortion winding (m_0 is distortion strength). The colours illustrate its non-uniform spatial mass modulation[157]. Panel **e** reproduced with permission from ref. 157, Springer Nature Ltd.

feature exotic band degeneracies, such as Dirac and Weyl points[22,54–57], quadratic and higher-order dispersions[58], nodal lines[59,60] and their varieties[61–63]. Associated with these degeneracies, lower-dimensional Fermi arcs connecting their projections are manifested as robust topological edge states.

As discussed, the robustness feature of topological photonic and acoustic systems is linked to a symmetry, be it time-reversal or spatially introduced lattice symmetry that protects the corresponding topological invariant, which is defined based on the integration of the Berry curvature associated with the band structure of conventional systems as summarized above (Fig. 1a). However, in other less conventional configurations, the process of defining a symmetry-related topological invariant differs from the standard approach (Fig. 1b–e). For example, in non-Hermitian, nonlinear and non-Abelian systems, the topological features cannot be characterized based on the standard linear band topology, as the band structures of such systems contain complex-valued eigenvectors, multiple entangled bandgaps or simply cannot be characterized based on Bloch band theory, the same as for real-space topological defects lacking global translation symmetry. To overcome these challenges, numerous studies have been carried out to investigate the topological characteristics of the aforementioned non-standard systems, leading to a second wave of topological phenomena in photonic and acoustic settings, which are summarized in this Review. We believe that our Review provides a timely survey of this fast-growing field and thus serves as a guide covering technical details and discussing future directions. We summarize the developments in non-Hermitian topology, nonlinear topology and non-Abelian topology, discuss topological defects, and finally provide an outlook.

Non-Hermitian topology

Studies on TIs in gainless and lossless systems ruled the early beginnings of photonic and acoustic advances, which have now been thoroughly broadened by the notion of non-Hermitian topology[64]. Non-Hermiticity represents energy exchanges with the ambient environment and is ubiquitous in open systems. Owing to the loss of Hermiticity, the eigenvalues of a non-Hermitian system typically become complex and the eigenvectors lose their orthogonality, accordingly, leading to intriguing non-Hermitian topological properties that modify or sometimes even profoundly change the otherwise Hermitian topology. In this section, we review the recent advances in this growing field.

For Hermitian systems, the energy (or frequency) dispersion relation is critical for determining topological phenomena[53]. Regarding the non-Hermitian counterparts, the bands play an equally important role, but, owing to their complex nature, the definitions become less straightforward compared with the Hermitian counterpart. Primarily, the bandgaps of the eigenenergies in the complex plane distribute in either a line-like or a point-like fashion[64]. If the complex band spectra of a non-Hermitian Hamiltonian $H(k)$ are separated by a baseline l_B, the system has a line gap. In contrast, $H(k)$ contains a point gap if a complex base (Fermi) energy E_B exists such that $\det[H(k) - E_B] \neq 0, \forall k$ within the Brillouin zone, where k denotes the wavevector (see Box 1 for details).

It has been proven that any non-Hermitian Hamiltonian with line gaps can be continuously deformed into either a Hermitian (for real) or an anti-Hermitian (for imaginary line gaps) matrix[64,65]. Correspondingly, the non-Hermitian system inherits topological properties from its Hermitian counterpart and the topological invariant can therefore also be determined following the Hermitian scheme upon proper

Box 1

Non-Hermitian bandgaps

Consider two periodic lattices whose non-Hermiticity comes from the on-site gain and loss (panel **a**) and the asymmetric couplings (panel **b**). The first lattice hosts complex line gaps, which can be further classified into real and imaginary ones (panel **c**). The second lattice, however, permits special point gaps even if there is only one band (panel **d**). These two non-Hermitian lattices represent two general classes that can be engineered in photonics or acoustic systems. Although loss is ubiquitous in absorbing materials, gain and asymmetric couplings require additional design sophistications. For example, pumping in semiconductors leads to optical gain[179] and amplitude and phase modulation give rise to asymmetric couplings[86]. Sonic gain, however, has been achieved using acoustic-electric devices[93] or electro-thermoacoustic coupling[82]. Thus, the shape of the complex bandgaps enables a systematical topological classification and provides a theoretical guideline to understand non-Hermitian TIs.

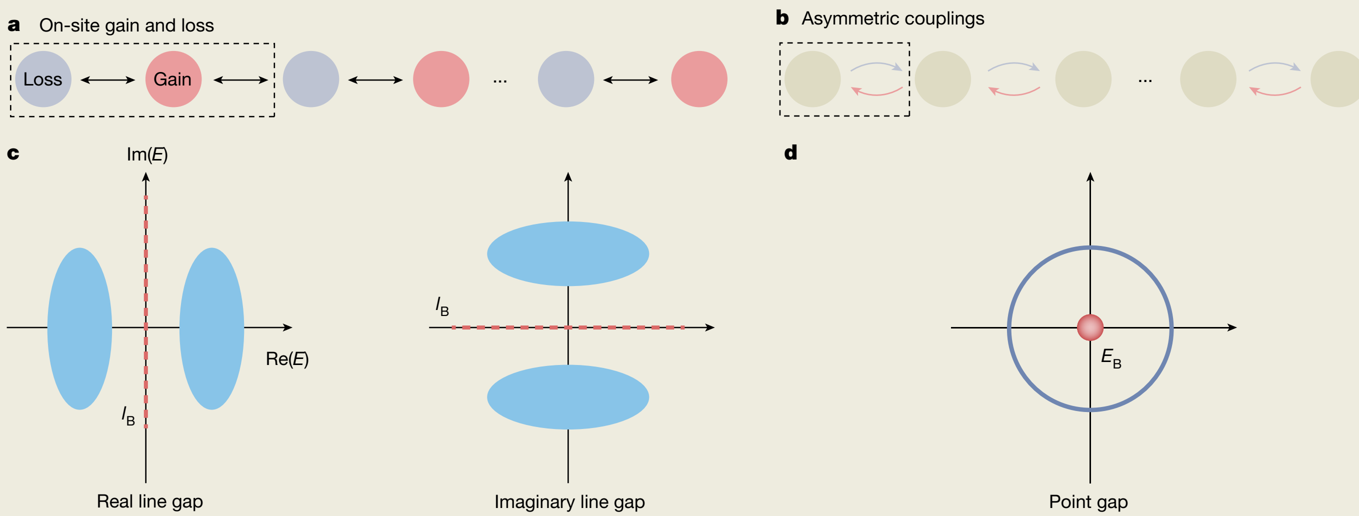

transformation. For example, it has been shown that a Su–Schrieffer–Heeger (SSH) model[66] with on-site gain and loss still supports mid-gap edge states characterized by the non-trivial Zak phase, similar to its Hermitian counterpart[67–69]. The difference is that the edge states become amplifying or lossy[67,70] (yet in a parity–time (PT) symmetric system, they may remain real[69]). Taking advantage of the topological robustness, non-Hermitian edge states have inspired extensive investigations in photonics and acoustics to connect those interfacial waves with lasing action (Fig. 2a). In photonics, it has been shown that non-Hermitian edge states can exhibit enhanced visibility and high stability during lasing[71–81]. In acoustics, efforts have been made to realize sasers (the acoustic version of lasers), relying on non-Hermitian TIs with electro-thermoacoustic couplings as the acoustic analogue of gain[82] (Fig. 2b).

Unlike line gaps, zero-dimensional point gaps enable special eigenenergy windings (Box 1), which give rise to novel band topology that is unique to non-Hermitian systems and responsible for a host of phenomena such as the non-Hermitian skin effect (NHSE)[83], complex-energy braiding[84–86] and even gapless exceptional features[87]. The NHSE is an effect that is attributed to an almost complete localization of all eigenstates at boundaries when driven by non-Hermiticity[88,89], which originates from their complex windings[83] (note that recently a type of NHSE without energy windings was discussed[90]). Again, photonics and acoustics platforms have shown ways to implement this effect[91–93]. For example, by applying time modulation to an optical fibre loop, asymmetric couplings are obtained for photons, giving rise to the NHSE where light is asymmetrically transported and funnelled to desired locations (Fig. 2c).

The complex-energy twisting and braiding (Fig. 2d) have been recently found to form braid groups and even carry non-Abelian features[84,86], which is discussed in the section 'Non-Abelian physics in photonic and acoustic systems'. Often, band twisting and braiding involve energy windings related to the point gaps. However, it was soon realized that owing to the multiband nature, only a small fraction of the braided bands have well-defined point and line gaps, suggesting the need for a more advanced homotopy theory[84,85,94]. These advancements only assume band separation[95] and thus provide a more general characterization of the non-Hermitian bands using braid groups, which complements the point- and line-gap schemes.

Another emerging branch focuses on the gapless non-Hermitian degeneracies, which unlike the Hermitian counterpart, can be driven towards a phase exhibiting footprints of exceptional characteristics[96–98]. Such features likewise fall within the scope of non-Hermitian band topology that can be characterized via the point- and line-gap scheme[87] or the homotopy theory[84]. For example, Fig. 2e exemplifies a Weyl exceptional ring associated with simultaneously coalesced eigenvalues and eigenvectors when scattering loss is added into a photonic waveguide array. In general, using various lattice symmetries, non-Hermitian degeneracies materialize in a plethora of guises, including exceptional points, lines and rings and even complex links[99–103], even in the context of the NHSE[104,105]. Therefore, combining non-Hermitian components with topology remains a thriving arena for studies of sound and light, and it is expected that the ability to engineer both periodic and aperiodic artificial systems[106] will stimulate ongoing fundamental and applied activities.

Nonlinear topology

Most of the proposed topological structures share a common property: from a system point of view, they are linear, obeying the so-called superposition principle[107]. Nonlinearity, however, is a common feature of many physical systems, which can lead to interesting effects such

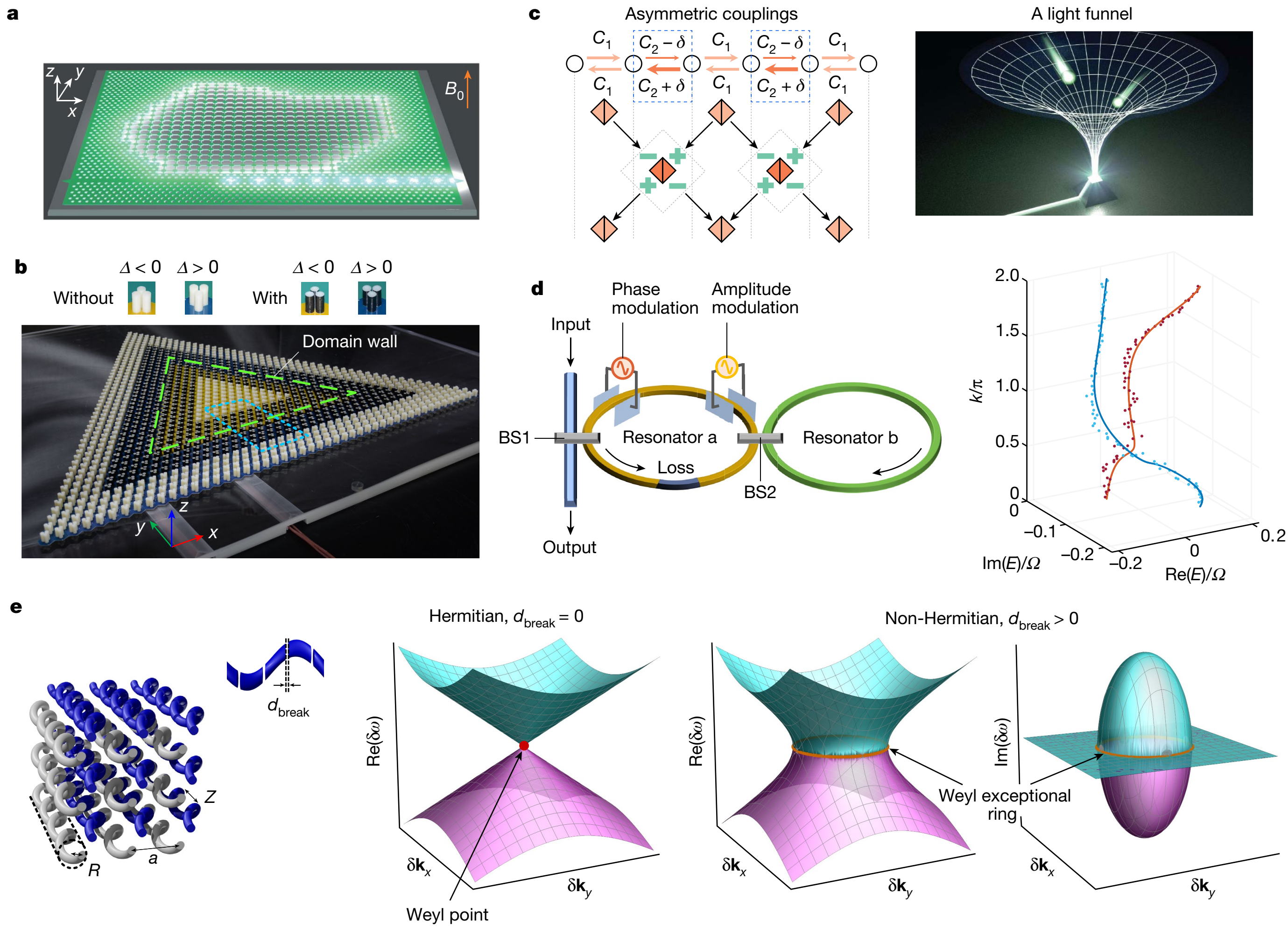

Fig. 2 | Non-Hermitian topological phenomena. a,**b**, Examples of photonic and acoustic topological lasers. The non-trivial lattice topologies are set to execute gain through stimulated emission and thermoacoustics, for the optical (**a**) and sonic (**b**) implementations[72,82]. B_0 denotes the magnetic field and Δ the geometry perturbations. **c**, The NHSE and a light funnel have been demonstrated in systems with asymmetric couplings and non-Hermitian point-gap topology[91]. $C_{1,2}$ represent the inter- and intracell couplings, with δ the non-Hermitian perturbation. **d**, Complex-energy braiding in a photonic ring-resonator design with amplitude and phase modulators has been designed to showcase non-Abelian features[86]. BS1 and BS2 are two beamsplitters; E denotes the complex eigenenergy of the coupled-resonator system; and Ω is the free spectral range of the resonators. **e**, A Weyl exceptional ring spreading from a Hermitian Weyl point takes place by introducing scattering loss into a photonic helical waveguide array[100]. d_{break} indicates the length of the breaks in the helical waveguides; R is the radius of the helix; Z and a are, respectively, the vertical and horizontal helix periods. Panels reproduced with permission from: **a**, ref. 72, AAAS; **b**, ref. 82, Springer Nature Ltd; **c**, ref. 91, AAAS; **d**, ref. 86, Springer Nature Ltd; **e**, ref. 100, Springer Nature Ltd.

as harmonic generation, self-focusing and solitonic propagation[108], none of which can occur in linear domains. For this reason, over the past few years, tremendous attention has been paid to the interplay between nonlinearity and topological physics, opening the research field of nonlinear TIs[109].

The existence of nonlinearities in a system poses challenges for the theoretical understanding of TIs and their edge states. In fact, when the nonlinearities become strong, the modal solution of a periodic structure can no longer be characterized using a Bloch-like function, preventing one from defining a band structure, from which, conventionally, a topological invariant can be defined. As such, active research is ongoing to understand the topological properties of photonic and acoustic systems in the nonlinear domain.

Compared with conventional linear topological structures, nonlinear TIs provide inherent reconfigurability. In particular, the nonlinear behaviour of such kinds of topological systems implies the dependence of the dynamics of their edge states on the excitation intensity. This feature offers a unique external control over not only topological phase transitions but also the characteristics of the corresponding in-gap edge states. This property paves the way towards the next generation of reconfigurable photonic and acoustic devices with topological features.

Reference 110 demonstrates a genuine nonlinearity-induced photonic TI, based on a bipartite square lattice of coupled optical waveguides, shown in Fig. 3a. The lattice features alternating linear and nonlinear couplings. The nonlinear coupling is achieved by introducing a detuning between the effective refractive indices of the optical waveguides. This forces a certain fraction of light to remain in the initially excited guide at all times, leading to a Kerr-type nonlinearity. In the linear regime (low power), the lattice structure remains topologically trivial. Yet, as the optical power is increased, the system is driven into the topologically non-trivial regime above a certain power threshold. This results in a power-dependence output intensity of the system, as shown in Fig. 3b. When launching low-power light at $P = 100$ kW into the edge waveguide (left panel), the light diffracts into the bulk of the lattice, leading to a low transfer ratio. In contrast, when the input peak power is increased to $P = 3.5$ MW (right panel), the system is derived into the topologically non-trivial phase, leading to the suppression

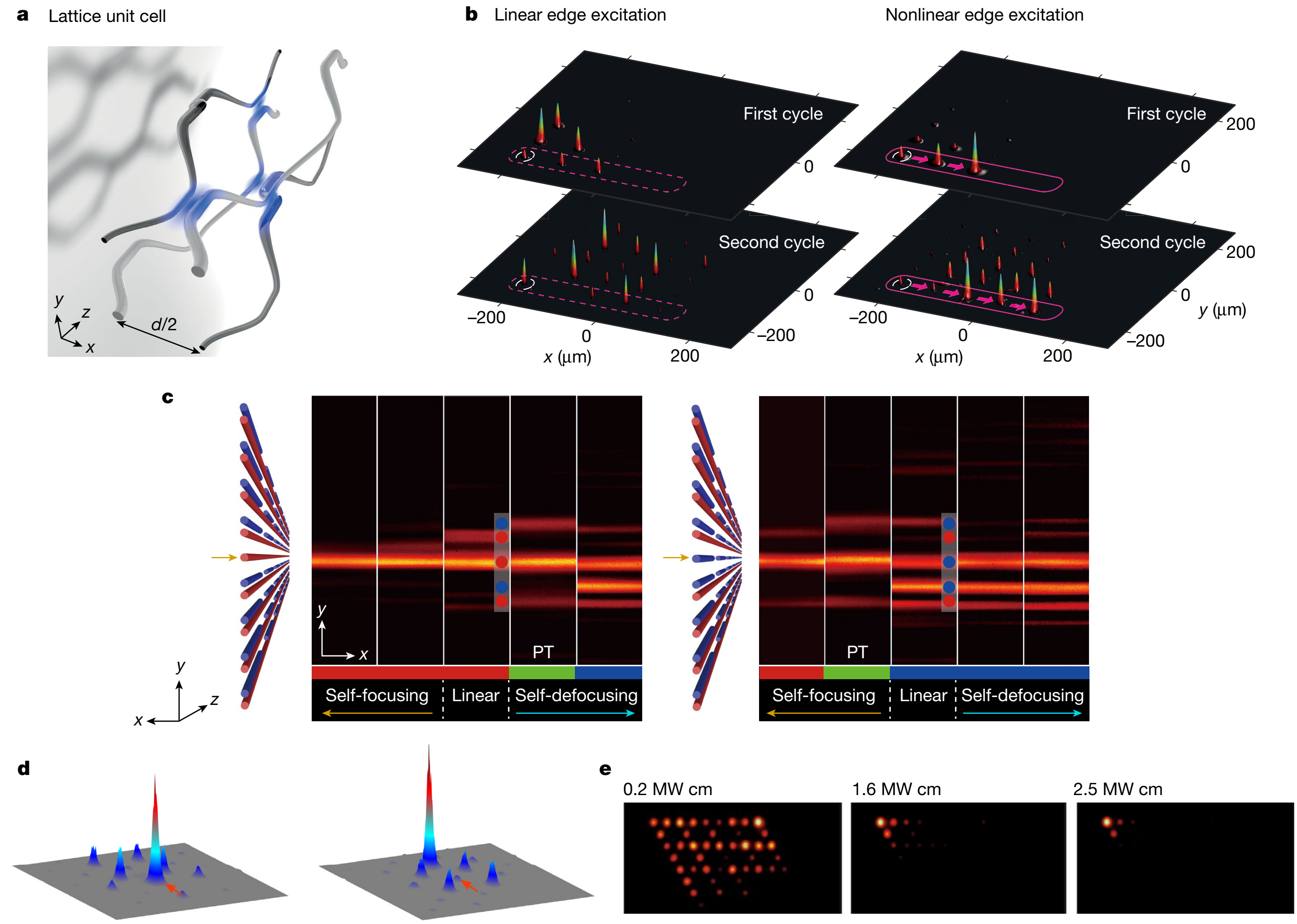

Fig. 3 | Nonlinearity-induced topological structures. a, Demonstration of a two-dimensional nonlinear photonic TI, based on coupled optical waveguides with detuned refractive index, enabling a Kerr-type nonlinearity. *d*, lattice constant. **b**, In the low-power regime, the light diffracts into the bulk of the lattice. For high values of the input power, however, the system is derived into a topologically non-trivial phase, leading to the formation of a chiral edge channel. **c**, Non-Hermitian topology: a non-Hermitian topological SSH model based on coupled optical waveguides, in which the gain and loss are controlled with nonlinearity. The active control of the loss and gain switches the system between PT- and non-PT-symmetric regimes. The transition between the PT- and non-PT-symmetric regimes is accompanied by destruction and restoration of the topological zero-energy mode with gainy (left) and lossy (right) interfaces[113]. **d**, Formation of an optical solitonic wave along the edge of a Floquet TI[114]. **e**, Formation of a nonlinearity-induced corner mode at the corner of a second-order TI with nonlinear effects[118]. Panels adapted with permission from: **a**,**b**, ref. 110, AAAS; **d**, ref. 114, AAAS; **e**, ref. 118, under a Creative Commons licence CC BY 4.0. Panel **c** reproduced with permission from ref. 113, AAAS.

of the undesired bulk diffraction and the formation of desired chiral edge channel.

Nonlinear topological structures have also been studied in phononics. In a mechanical setting[111], the nonlinearity management of an SSH-like mass–spring system was reported, consisting of masses connected with two types of nonlinear spring with stiffening and softening types. The nonlinear coupling drives the system into a topologically non-trivial phase in the regime of high-intensity power. Likewise, in ref. 112, a tunable nonlinear acoustic topological system was proposed based on the same principle. These proposals promise to enable a generation of reconfigurable and robust topological devices. Beyond this, the extension of topological ideas to the nonlinear realm enables a large variety of unprecedented physical phenomena that have no counterparts in the linear domains, some of which are briefly discussed in the following section.

Emerging topics in nonlinear topology

The structure described in Fig. 3a was made from passive elements, corresponding to a Hermitian Hamiltonian. Recently, the concept of nonlinear TIs has been extended to the realm of non-Hermitian systems, including active elements and featuring interesting phenomena such as PT symmetry[96]. Similar to the Hermitian case, nonlinear effects in non-Hermitian TIs can be leveraged as a tuning knob to control the properties of the corresponding topological edge states. In ref. 113, the possibility of controlling PT symmetry and the corresponding non-Hermitian topological edge states is demonstrated in a photonic TI. This is achieved based on a non-Hermitian SSH lattice, consisting of gainy (γ) and lossy ($-\gamma$) waveguides and an interface defect. The optical nonlinearity changes the real part of the refractive index of the waveguides, enabling active control of the loss and gain of the non-Hermitian SSH lattice, switching it between PT-symmetric and non-PT-symmetric regimes. The transition between the PT-symmetric and non-PT-symmetric regimes is accompanied by destruction and restoration of the topological zero-energy mode. This phenomenon is observed in Fig. 3c, illustrating the nonlinear restoring of topological states in an initially non-PT lattice that is truncated with a gainy (left panel) or a lossy (right panel) interface.

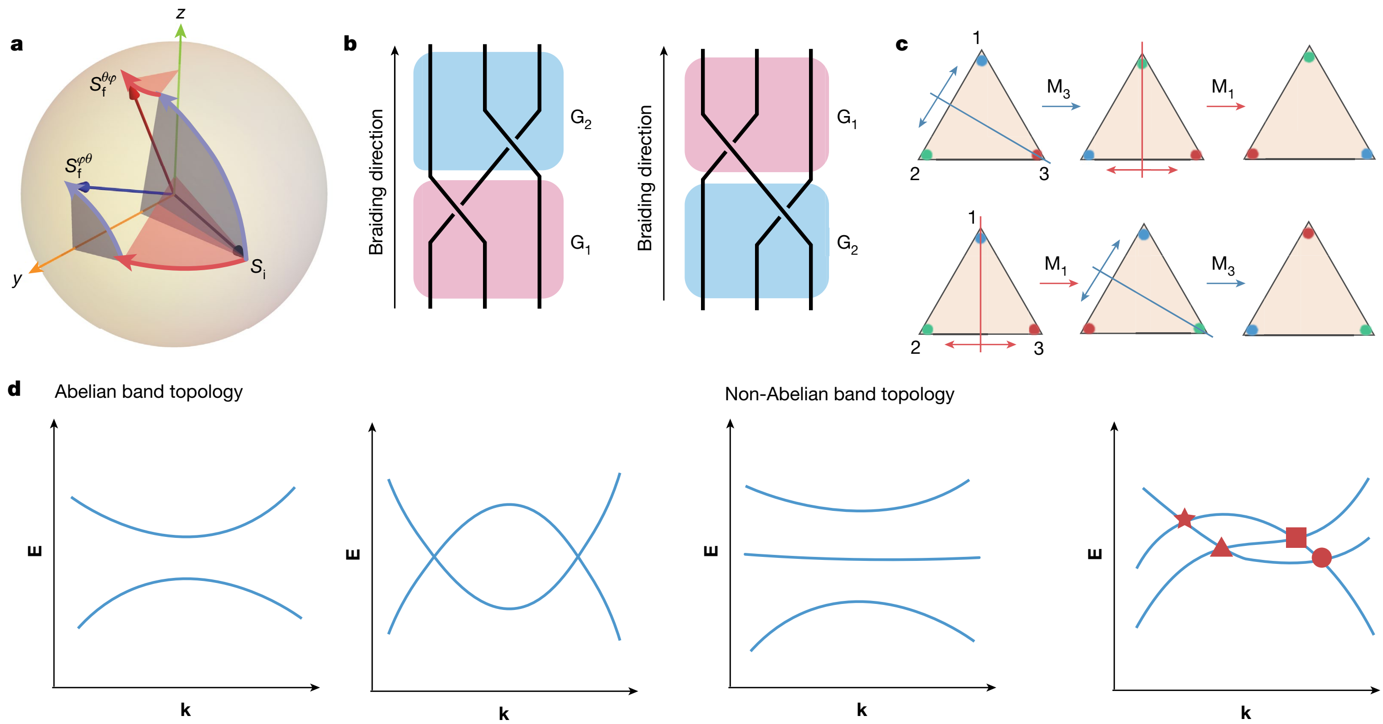

Fig. 4 | Non-Abelian wave physics. With high-dimensional parameter space employed, the evolution operators are no longer commutative, indicating non-Abelian structures. As examples, these physical operators can be elements of an abstract. **a**, SU(2) group, wherein temporal modulation (φ rotation around y axis) and the Faraday effect (θ rotation around z axis) contribute to the two rotation operators (S_f) acting on the initial state S_i. **b**, A braid group B_3, in which state evolutions along certain parameter loops manifest as braid operators, represented by G_1 and G_2. **c**, A permutation group, D_3, wherein the permutation operators (geometrically demonstrated as mirror operations M_1 and M_3) are eigenstates exchanging in a non-Hermitian system. **d**, In contrast to a two-band model captured by an Abelian topological invariant, multiple entangled bands with real eigenfunctions involve non-Abelian band topology. The symbols indicate band nodes characterized by non-Abelian group elements. Panel **a** adapted with permission from ref. 119, AAAS.

Another interesting phenomenon related to nonlinear TIs is solitonic wave propagation alongside the corresponding edge states, which happens when the nonlinear effects compensate for the dispersive effects in the system. Figure 3d shows an example of solitonic wave propagation with topological features, demonstrated in ref. 114 based on an array of periodically modulated waveguides designed to realize a Floquet-type photonic TI. In the presence of nonlinearity, the optical Kerr effect leads to the formation of an optical solitonic wave, propagating without changing its shape along the edge of the topological structure (Fig. 3d). Topological edge solitons have been proposed and implemented in other reports[115,116]. Yet, active research is ongoing to understand the topological properties and robustness of such kinds of edge states, which cannot be simply characterized based on the band-topology definition in the linear systems. Furthermore, the extension of nonlinear topological systems to higher orders, characterized by a non-trivial bulk polarization is also an emerging direction. In ref. 117, nonlinear topology of second order was theoretically proposed, and afterwards demonstrated experimentally based on a photonic structure consisting of a rhomboidal kagome lattice[118]. Figure 3e shows the formation of gapless corner states, the hallmark of second-order topology, when the input power to the system increases, invoking the nonlinear effects. Such kinds of nonlinearity-induced corner modes open the door to exciting applications such as energy harvesting and lasing.

Non-Abelian physics in photonic and acoustic systems

Band topology is best displayed in terms of robust boundary responses, as discussed in the previous sections. Another example in band theory revealing robust behaviour associated with topology protection is the knot structure, which exhibits a complex set of topological invariants and is mathematically classified through non-Abelian groups. The non-Abelian groups feature non-commutativity of operations and are pervasive in physics. In this section, we review recent findings on how non-Abelian structures, including non-Abelian gauge fields, non-Abelian geometric phases and non-Abelian topological charges, emerge in classical wave systems. A common example to introduce non-Abelian operations is two rotations in three-dimensional spaces about the x and y axes. By mapping the rotation operation to a physical quantity (gauge field) and mimicking them in a real system, a non-Abelian gauge field emerges to entangle degenerate modes through external fields. A previous study utilized degenerate optical modes sequenced by two rotation operators to break the $\mathcal{T}$ symmetry and synthesize a non-Abelian gauge field, as shown in Fig. 4a, in which one rotation is the temporal modulation and the other is the Faraday effect[119]. In addition, by reinspecting the contribution of material parameter anisotropy, a wide class of anisotropic materials imitate a non-Abelian gauge field for two-dimensional optical waves[120]. Braiding is another non-Abelian operation and is of great significance for physics, as it is regarded as one promising way to achieve fault-tolerant topological quantum computing[121]. Exchanging two anyons in two dimensions can mimic the braiding operation, inducing a matrix-valued phase to the wavefunction relative to the initial state. Such a matrix-valued phase can be non-Abelian when three or more anyons are involved. Unfortunately, considerable technological challenges persist in observing anyons. Interestingly, parallel transport of two degenerate states in the parameter space along a quarter surface of a sphere reproduces the braiding operation[122]. Replicating the non-Abelian geometric phases by adiabatic evolution of multiple degenerate states is proposed in acoustics and arrays of laser-written waveguides to generate the unitary group[123] as well as the braid group[124,125], shown in Fig. 4b. In these classical systems, however, without the many-body topological protection, the chiral-symmetry-protected mode degeneracy is fragile and delicate in terms of its artificial structure designs. To circumvent the effects of structural imperfections, dynamically driving the degenerate modes through tunable external fields is a promising direction. Even without the perfectly degenerate modes, multiple-state evolution introduces non-Abelian behaviour such as non-Abelian Thouless pumping[125–127]. The non-Abelian property originates from the non-commutative combination of two distinct pump cycles between three states. The non-Abelian geometric phase also exits at a self-dual system, which affects the semiclassical propagation of wavepackets and leads to non-commuting mechanical responses[128]. Moreover, topological braiding of complex-energy bands is possible owing to state exchange encircling multiple exceptional points in non-Hermitian systems, wherein diverse knot-structured energy spectra have been observed[86,129,130], as shown in Fig. 2d. Also, permutation groups can be non-Abelian. A closed loop around an exceptional point is accompanied by state permutations[131]. For instance, the permutation forms the element of the dihedral group which is also non-Abelian, as illustrated in Fig. 4c.

In addition to exploring non-Abelian phenomena based on manipulating states, researchers reinspected the topological invariant in band physics and found non-Abelian structures. A single bandgap or band node can be characterized by a topological invariant, with tenfold classification being a prime example[132]. The symmetry underlying a structure further enriches the classification, in which the topological invariants are usually classified into Abelian groups. Rooted in the Abelian character, common wisdom holds that band and bandgap topology are linked to each other by simple addition, and the Weyl points can annihilate with different chirality. Both are challenged by the introduction of non-Abelian band topology based on multiband descriptions instead of a single band.

The scope of topological effects associated with Dirac or Weyl points, characterized by Abelian topological invariants, can be further advanced by considering nodal-line metals with multiple bands. Research reveals the non-Abelian charge of band nodes[133]. In the presence of certain symmetries (combination of space-inversion or rotation and $\mathcal{T}$ symmetry), the eigenstates are real-valued, indicating trivial topology in the previous frameworks. Nevertheless, the space of available Hamiltonians to stabilize the nodal lines is characterized by these real eigenstates space, giving additional classifications to distinguish the Hamiltonians. A powerful mathematical tool to classify these spaces is the fundamental group, which can be Abelian or non-Abelian, associated with the number of involved bands, as shown in Fig. 4d. It is noted that the idea is also applied to classify non-Hermitian band topology as well[84]. In the simplest one-dimensional three-band model, the fundamental group of the eigenstate space is isomorphic to $\pi(O(3)/O(1)^3) = Q$, where $O(3)$ is the orthogonal group spanned by the real eigenfunctions, $O(1)$ represents the gauge freedom, and Q forms a non-Abelian quaternion group. Such non-Abelian characteristics induced by collective consideration of multiple bands are possible to manifest more complex scenarios. Prominent examples include non-trivial bandgaps and corresponding edge states in one-dimensional systems beyond the Zak phase description[134], and non-Abelian band nodes and the patch Euler class in the two-dimensional systems[135–139]. In three dimensions, the salient feature of non-Abelian topological protection is transferred to the emergence of various admissible nodal-line configurations such as nodal chain[140], nodal ring[61] and nodal earring[141]. In particular, the theory based on multiband description predicts non-Abelian topological charges, which arise upon braiding the nodes inside the momentum space[142]. The interplay of the non-Abelian topology with space symmetries enables topological phase transitions in which pairs of Weyl points may scatter or convert into nodal-line rings, liberated from fundamental constraints based on Abelian band topology, which predicts that two Weyl points will annihilate with different chirality. The richness of non-Abelian physics offers substantial unexplored opportunities, where topological effects can emerge. Of particular interest is the bulk–boundary correspondence: as the non-Abelian charge is not an integer compared with the Chern number, its correspondence to the number of edge states is not obvious. Although its generalization to non-Abelian regions is already exemplified[134,143], strict mathematical certification is still an ongoing challenge.

Topological defects

We learned that when defects are introduced to the topological lattice while the underlying symmetry is not ruptured, confined edge or corner states prevail. In this section, we do not focus on the non-trivial resilience against the added defects; instead, we focus on topological defects in an otherwise perfect crystal. These topological defects are labelled as such because no lattice rearrangement or continuous deformation can fix them as they constitute local kinks or obstructions in an order parameter field. Typically, these defects contain a core where the order is destroyed and an outer zone of slowly varying variables[144,145]. We label defects depending on the type of symmetry that is broken. For example, disclinations and dislocations break with the rotational and translational lattice symmetry, respectively, and are found to be plentiful in nature. The stripe pattern of a zebra indeed has those two defect types: disclinations are seen in the changes of the stripe orientations around its limbs, whereas dislocation 'pitchforks' are present where new stripes seem to split the order, as shown in Fig. 5a. Other prominent examples are grain boundaries that are topological line defects between crystallites as in polycrystalline graphene[146] and topological vortices that can bind Majorana bound states to the vortex core in topological superconductors[147].

In the previous sections, we reviewed systems governed by the bulk–boundary correspondence and the non-Bloch version of it, which are at the core of topologically robust states, respectively, ruling the Hermitian and non-Hermitian non-trivial interface confinements. Topological defects, in contrast, constitute an extension thereof, in that the real-space topology of the specific defect plays a pivotal role in connection with the underlying band topology in reciprocal (momentum) space[148–152]. Hence, a modification of the conventional bulk–boundary correspondence pertains to specific bulk-defect correspondences, which we expand on in the following.

Defects as in superfluids and topological superconductors are of the vortex type that cannot be destroyed by a continuous deformation of the order parameter[147,153]. For example, a singular vortex carries a quantized magnetic flux that can be characterized by a real-space winding number, which shares a similar origin to the non-zero Berry phase in non-trivial TIs. The Jackiw–Rossi model, describing how a zero mode can bind to the vortex core, was originally conceived in quantum field theory and subsequently discussed in graphene in the context of a topological midgap state in the Dirac spectrum[154,155]. It was shown that by adding a gap-opening parameter in the form of a vortex, a topological zero-energy state becomes trapped at the vortex core. Later it was shown that this concept can be mapped onto magnetic flux vortices in spinless, p-wave superconductors[156]. As the seminal finding was explored in a single-particle scenario, it did not take much time until entirely classical zero-mode analogies were unearthed[157]. Researchers took an acoustic approach towards this type of topological vortex defect at which a sonic zero-mode is pinned[158,159]. By 3D-printing a plastic lattice to emulate graphene's Dirac spectrum, a so-called Kekulé texture provided the necessary spatial mass modulation to form a vortex incorporating an angular phase winding, as shown in Fig. 5b. In doing so, a sonic bound state remains topologically pinned to the acoustic Dirac frequency, regardless of any particle–hole symmetry-preserving defects introduced. Using steel bolts on a plate arranged in a honeycomb pattern established the basis for the

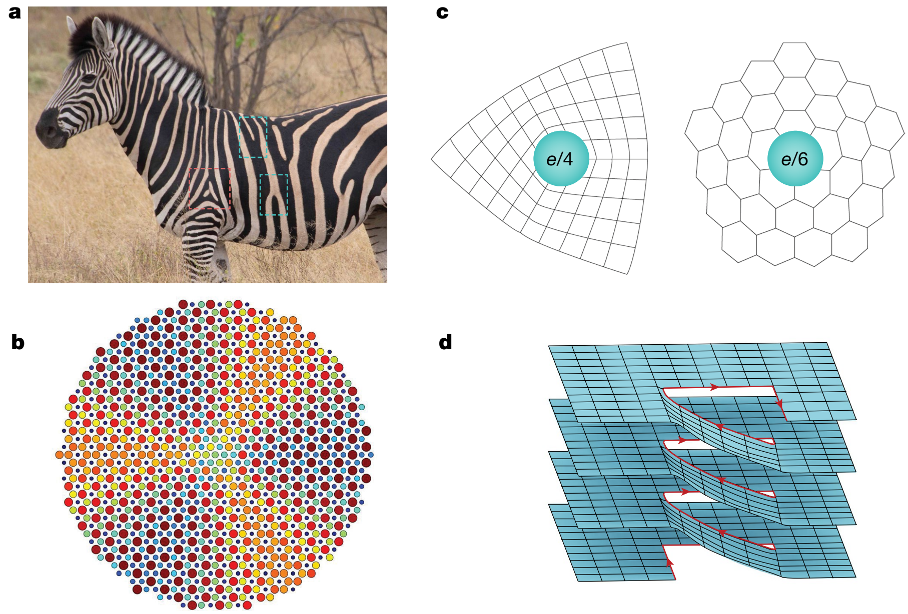

Fig. 5 | Topological defects. a, Topological disclination (red box) and dislocations (blue boxes) displayed in nature on a zebra's stripes. **b**, Illustration of an acoustic Jackiw–Rossi vortex comprising a Kekulé radii texture in a finite triangular sonic lattice[158]. Such a topological vortex has been explored both using photonics and acoustics lattice settings. **c**, Topological disclination defects in a square and a hexagonal lattice trapping a fractional charge quantized in units of $e/4$ and $e/6$, respectively[168,169]. **d**, Illustration of a screw dislocation comprising the cut-and-glued planes in three dimensions[152]. Panels adapted with permission from: **a**, David Minty (https://www.flickr.com/photos/its_all_about_the_light/44762387315/sizes/l/), under a Creative Commons licence CC BY 2.0; **c**, ref. 178, Springer Nature Ltd; **d**, ref. 152, Springer Nature Ltd. Panel **b** reproduced with permission from ref. 158, APS.

Kekulé-distorted mechanical vortex implementation through flexural mode vibrations[160]. At higher megahertz frequencies, a similar approach has been implemented, but also considering an auxiliary orbital degree of freedom and nonlinearities[161]. An equally exciting avenue concerning topological vortex defects has been paved using light. Employing femtosecond laser direct writing to create waveguide lattices and electron-beam lithography to textured triangular perforations in a silicon layer has successfully led to near-infrared topological zero modes and a Dirac-vortex topological-cavity surface-emitting laser at telecommunication wavelengths, respectively[80,162,163]. Furthermore, as discussed in the previous section, non-Abelian braiding of vortices can be carried out and even bound vortex light in association with emulated cosmic strings is possible[164,165].

The bulk–disclination correspondence links lattice bulk topology with the real-space topological defect charge and has recently led to the observation of fractional charges trapped at defects lacking rotation symmetry. Broadly speaking, topological crystalline insulators have exhibited a wealth of quantized phenomena, among which zero-dimensional localized states are quantized in fractions of the elementary electronic charge (e)[166,167]. Thus, in addition to the topology features of the band structure, the Frank angle and the Burgers vector, which characterize the disclination defects by their rotation and translation, respectively, enable insight into their topological interplay, and, more importantly, can be used to determine the fractional disclination charge, as reported in two contributions on topological crystalline insulators using a microwave metamaterial[168] and a photonic crystal approach[169]. In the former experiment, it was found that the charge quantizes in units of $e/4$ in a square lattice, and in the latter, in units of $e/6$ using a hexagonal lattice (Fig. 5c). In the absence of fractional charges, researchers engineered disclinations in acoustic lattices with topological midgap states protected by chiral symmetry[170]. Recently, a topological valley Hall phase has also been incorporated with human-made disclinations using both photonic and elastic configurations[171,172].

Dislocations, as briefly mentioned above, are topological defects that owing to the conservation of the Burgers vector cannot be removed through local perturbations. The two types are edge dislocations that run perpendicular and the screw dislocations that run parallel to its Burgers vector. Interestingly, a study discussed how lattice dislocations of the latter type in so-called weak three-dimensional TIs can host gapless helical modes, closely resembling the ones from a two-dimensional quantum spin Hall insulator[152]. Evidence of such bulk–dislocation correspondence was provided with two back-to-back acoustic experiments using 3D printing and a cut-and-glue approach (or Volterra process) to create the helical defect along which the acoustic dislocation modes spiral[173,174]. Another recent experiment took a photonic route at optical frequencies[175]. Lastly, other planar defects include the domain walls (similar to grain boundaries), which have been synthesized in intersecting sonic lattices that flank a topological corner excitation[176]. Also, another promising avenue constitutes fractal photonic TIs whose self-similar topology features increased velocities compared with conventional TIs[177].

Outlook

In this Review, we addressed a focused scope of research avenues that marks the most recent frontiers in topological studies comprising light and sound. The way this field has emerged still seems to be its main driving force. Topological classical waves using human-made acoustical and photonic lattices rose to popularity in a close race with its forerunner frontier of topological quantum materials. What seemed to be hard, even impossible at times, to explore in topological quantum materials often stimulated a surge to emulate the equivalent classical analogy using sound or light. Compared with electronic materials, artificial acoustic and photonic bandgap materials have non-equilibrium characteristics and their band structure is not constrained by Fermi levels. Furthermore, these classical lattices have the advantages of flexible structure adjustability, easy manufacturing and measurement. Therefore, this frontier has grown to become an appealing platform to unravel fundamental topological physics with practical implementations yet to be unearthed. In this spirit, as we covered throughout this

Review, we have witnessed numerous wave-based advances focusing on the non-Hermitian, nonlinear and non-Abelian aspects of topology, including deterministically engineered topological defects. It is thus foreseeable that the lessons learned in creating topological phases of robust guiding of sound and light will become a priority topic among scientists and engineers aiming at taking an application-oriented route.

The unique band topology of photonic and acoustic lattices, particularly in two dimensions, provides a host of technical opportunities owing to their most representative phenomena such as the quantum Hall or valley Hall effects, which provide a novel topological waveguide scheme comprising suppressed reflection of sound or light. The attributes that are associated with the advantageous form of guiding waves pertain to spin–momentum locking, backscattering suppression, free-path steering, strong defect immunity and multi degree-of-freedom regulation, which have the potential to revolutionize photonic and acoustic devices. Energy transportation systems based on topological waveguides offer much higher robustness than traditional waveguides. Resonators realized using topological ring waveguides and higher-order topological corner insulators are both wave-confining systems with potential applications for energy harvesting. These advantages provide a feasible technical path for improving the robustness of various acoustic (kilohertz to gigahertz) and photonic (gigahertz to petahertz) resonators, filters, delay-line devices, routers, circulators, opto-acoustic modulators, lasers, directional emitters and so on.

Beyond these more tangible directions, there are also many other important aspects emerging in this research field, in particular providing possibilities for the development of topological quantum information. Although a direct link between this topic and classical topology, rightfully spoken, seems obscure, a light- or sound-based understanding of topological quantum computation may lead to deeper insight into non-Abelian geometric phases, anyon-like statistics, concatenated operations and holonomic transformations.

Tangible and conceptual questions still remain at the forefront of current activities concerning topological sound and light control. What started as a curiosity-driven undertaking, has seriously expanded into influential exploration on geometry-induced and protected wave-based properties to take the next generation of devices by storm.

1. Engheta, N. & Ziolkowski, R. W. *Metamaterials: Physics and Engineering Explorations* (Wiley, 2006).
2. Cummer, S. A., Christensen, J. & Alù, A. Controlling sound with acoustic metamaterials. *Nat. Rev. Mater.* **1**, 16001 (2016).
3. Hasan, M. Z. & Kane, C. L. Colloquium: topological insulators. *Rev. Mod. Phys.* **82**, 3045–3067 (2010).
4. Qi, X.-L. & Zhang, S.-C. Topological insulators and superconductors. *Rev. Mod. Phys.* **83**, 1057–1110 (2011).
5. Lu, L., Joannopoulos, J. D. & Soljacić, M. Topological photonics. *Nat. Photon.* **8**, 821–829 (2014).
6. Zhang, X., Xiao, M., Cheng, Y., Lu, M.-H. & Christensen, J. Topological sound. *Commun. Phys.* **1**, 97 (2018).
7. Xie, B.-Y. et al. Photonics meets topology. *Opt. Express* **26**, 24531–24550 (2018).
8. Ma, G., Xiao, M. & Chan, C. T. Topological phases in acoustic and mechanical systems. *Nat. Rev. Phys.* **1**, 281–294 (2019).
9. Ozawa, T. et al. Topological photonics. *Rev. Mod. Phys.* **91**, 015006 (2019).
10. Thouless, D. J., Kohmoto, M., Nightingale, M. P. & den Nijs, M. Quantized Hall conductance in a two-dimensional periodic potential. *Phys. Rev. Lett.* **49**, 405–408 (1982).
11. Haldane, F. & Raghu, S. Possible realization of directional optical waveguides in photonic crystals with broken time-reversal symmetry. *Phys. Rev. Lett.* **100**, 013904 (2008).
12. Wang, Z., Chong, Y. D., Joannopoulos, J. D. & Soljacić, M. Observation of unidirectional backscattering-immune topological electromagnetic states. *Nature* **461**, 772–775 (2009).
13. Fleury, R., Sounas, D. L., Sieck, C. F., Haberman, M. R. & Alù, A. Sound isolation and giant linear nonreciprocity in a compact acoustic circulator. *Science* **343**, 516–519 (2014).
14. Ni, X. et al. Topologically protected one-way edge mode in networks of acoustic resonators with circulating air flow. *New J. Phys.* **17**, 053016 (2015).
15. Yang, Z. et al. Topological acoustics. *Phys. Rev. Lett.* **114**, 114301 (2015).
16. Khanikaev, A. B., Fleury, R., Mousavi, S. H. & Alu, A. Topologically robust sound propagation in an angular-momentum-biased graphene-like resonator lattice. *Nat. Commun.* **6**, 8260 (2015).
17. Rechtsman, M. C. et al. Photonic Floquet topological insulators. *Nature* **496**, 196–200 (2013).
18. Yang, Z., Lustig, E., Lumer, Y. & Segev, M. Photonic Floquet topological insulators in a fractal lattice. *Light. Sci. Appl.* **9**, 128 (2020).
19. Peano, V., Brendel, C., Schmidt, M. & Marquardt, F. Topological phases of sound and light. *Phys. Rev. X* **5**, 031011 (2015).
20. Fleury, R., Khanikaev, A. B. & Alù, A. Floquet topological insulators for sound. *Nat. Commun.* **7**, 11744 (2016).
21. Rechtsman, M. C. et al. Strain-induced pseudomagnetic field and photonic Landau levels in dielectric structures. *Nat. Photon.* **7**, 153–158 (2013).
22. Xiao, M., Chen, W.-J., He, W.-Y. & Chan, C. T. Synthetic gauge flux and Weyl points in acoustic systems. *Nat. Phys.* **11**, 920–924 (2015).
23. Kremer, M. et al. A square-root topological insulator with non-quantized indices realized with photonic Aharonov–Bohm cages. *Nat Commun.* **11**, 907 (2020).
24. Kane, C. L. & Mele, E. J. Z_2 topological order and the quantum spin Hall effect. *Phys. Rev. Lett.* **95**, 146802 (2005).
25. Kane, C. L. & Mele, E. J. Quantum spin Hall effect in graphene. *Phys. Rev. Lett.* **95**, 226801 (2005).
26. Bernevig, B. A., Hughes, T. L. & Zhang, S.-C. Quantum spin Hall effect and topological phase transition in HgTe quantum wells. *Science* **314**, 1757–1761 (2006).
27. Mousavi, S. H., Khanikaev, A. B. & Wang, Z. Topologically protected elastic waves in phononic metamaterials. *Nat. Commun.* **6**, 8682 (2015).
28. Khanikaev, A. B. et al. Photonic topological insulators. *Nat. Mater.* **12**, 233–239 (2013).
29. Ma, T., Khanikaev, A. B., Mousavi, S. H. & Shvets, G. Guiding electromagnetic waves around sharp corners: topologically protected photonic transport in metawaveguides. *Phys. Rev. Lett.* **114**, 127401 (2015).
30. Wu, L.-H. & Hu, X. Scheme for achieving a topological photonic crystal by using dielectric material. *Phys. Rev. Lett.* **114**, 223901 (2015).
31. He, C. et al. Photonic topological insulator with broken time-reversal symmetry. *Proc. Natl Acad. Sci. USA* **113**, 4924–4928 (2016).
32. He, C. et al. Acoustic topological insulator and robust one-way sound transport. *Nat. Phys.* **12**, 1124–1129 (2016).
33. Maczewsky, L. J. et al. Fermionic time-reversal symmetry in a photonic topological insulator. *Nat. Mater.* **19**, 855–860 (2020).
34. Lu, J., Qiu, C., Ke, M. & Liu, Z. Valley vortex states in sonic crystals. *Phys. Rev. Lett.* **116**, 093901 (2016).
35. Dong, J.-W., Chen, X.-D., Zhu, H., Wang, Y. & Zhang, X. Valley photonic crystals for control of spin and topology. *Nat. Mater.* **16**, 298–302 (2017).
36. Lu, J. et al. Observation of topological valley transport of sound in sonic crystals. *Nat. Phys.* **13**, 369–374 (2017).
37. Gao, F. et al. Topologically protected refraction of robust kink states in valley photonic crystals. *Nat. Phys.* **14**, 140–144 (2018).
38. Xie, B. et al. Higher-order band topology. *Nat. Rev. Phys.* **3**, 520–532 (2021).
39. Benalcazar, W. A., Bernevig, B. A. & Hughes, T. L. Quantized electric multipole insulators. *Science* **357**, 61–66 (2017).
40. Ezawa, M. Higher-order topological insulators and semimetals on the breathing kagome and pyrochlore lattices. *Phys. Rev. Lett.* **120**, 026801 (2018).
41. Serra-Garcia, M. et al. Observation of a phononic quadrupole topological insulator. *Nature* **555**, 342–345 (2018).
42. Peterson, C. W., Benalcazar, W. A., Hughes, T. L. & Bahl, G. A quantized microwave quadrupole insulator with topologically protected corner states. *Nature* **555**, 346–350 (2018).
43. Xie, B. et al. Visualization of higher-order topological insulating phases in two-dimensional dielectric photonic crystals. *Phys. Rev. Lett.* **122**, 233903 (2019).
44. Chen, X.-D. et al. Direct observation of corner states in second-order topological photonic crystal slabs. *Phys. Rev. Lett.* **122**, 233902 (2019).
45. Xue, H., Yang, Y., Gao, F., Chong, Y. & Zhang, B. Acoustic higher-order topological insulator on a kagome lattice. *Nat. Mater.* **18**, 108–112 (2019).
46. Ni, X., Weiner, M., Alu, A. & Khanikaev, A. B. Observation of higher-order topological acoustic states protected by generalized chiral symmetry. *Nat. Mater.* **18**, 113–120 (2019).
47. Zhang, X. et al. Second-order topology and multidimensional topological transitions in sonic crystals. *Nat. Phys.* **15**, 582–588 (2019).
48. Zhang, Z. et al. Deep-subwavelength holey acoustic second-order topological insulators. *Adv. Mater.* **31**, 1904682 (2019).
49. Imhof, S. et al. Topolectrical-circuit realization of topological corner modes. *Nat. Phys.* **14**, 925–929 (2018).
50. Lee, C. H. et al. Topolectrical circuits. *Commun. Phys.* **1**, 39 (2018).
51. Bao, J. et al. Topoelectrical circuit octupole insulator with topologically protected corner states. *Phys. Rev. B* **100**, 201406 (2019).
52. Song, L., Yang, H., Cao, Y. & Yan, P. Realization of the square-root higher-order topological insulator in electric circuits. *Nano Lett.* **20**, 7566–7571 (2020).
53. Chiu, C.-K., Teo, J. C., Schnyder, A. P. & Ryu, S. Classification of topological quantum matter with symmetries. *Rev. Mod. Phys.* **88**, 035005 (2016).
54. Lu, L., Fu, L., Joannopoulos, J. D. & Soljačić, M. Weyl points and line nodes in gyroid photonic crystals. *Nat. Photon.* **7**, 294–299 (2013).
55. Lu, L. et al. Experimental observation of Weyl points. *Science* **349**, 622–624 (2015).
56. Li, F., Huang, X., Lu, J., Ma, J. & Liu, Z. Weyl points and fermi arcs in a chiral phononic crystal. *Nat. Phys.* **14**, 30–34 (2018).
57. Cai, X. et al. Symmetry-enforced three-dimensional Dirac phononic crystals. *Light. Sci. Appl.* **9**, 38 (2020).
58. He, H. et al. Observation of quadratic Weyl points and double-helicoid arcs. *Nat. Commun.* **11**, 1820 (2020).
59. Gao, W. et al. Experimental observation of photonic nodal line degeneracies in metacrystals. *Nat. Commun.* **9**, 950 (2018).
60. Qiu, H. et al. Straight nodal lines and waterslide surface states observed in acoustic metacrystals. *Phys. Rev. B* **100**, 041303 (2019).
61. Deng, W. et al. Nodal rings and drumhead surface states in phononic crystals. *Nat. Commun.* **10**, 1769 (2019).
62. Yang, Y. et al. Observation of a topological nodal surface and its surface-state arcs in an artificial acoustic crystal. *Nat. Commun.* **10**, 5185 (2019).

63. Xiao, M. et al. Experimental demonstration of acoustic semimetal with topologically charged nodal surface. *Sci. Adv.* **6**, eaav2360 (2020).
64. Kawabata, K., Shiozaki, K., Ueda, M. & Sato, M. Symmetry and topology in non-Hermitian physics. *Phys. Rev. X* **9**, 041015 (2019).
Theoretical framework for non-Hermitian topological phases.
65. Ashida, Y., Gong, Z. & Ueda, M. Non-Hermitian physics. *Adv. Phys.* **69**, 249–435 (2020).
66. Su, W., Schrieffer, J. & Heeger, A. J. Solitons in polyacetylene. *Phys. Rev. Lett.* **42**, 1698–1701 (1979).
67. Schomerus, H. Topologically protected midgap states in complex photonic lattices. *Opt. Lett.* **38**, 1912–1914 (2013).
68. Zeuner, J. M. et al. Observation of a topological transition in the bulk of a non-Hermitian system. *Phys. Rev. Lett.* **115**, 040402 (2015).
69. Weimann, S. et al. Topologically protected bound states in photonic parity–time-symmetric crystals. *Nat. Mater.* **16**, 433–438 (2017).
70. Zhang, Z., López, M. R., Cheng, Y., Liu, X. & Christensen, J. Non-Hermitian sonic second-order topological insulator. *Phys. Rev. Lett.* **122**, 195501 (2019).
71. Poli, C., Bellec, M., Kuhl, U., Mortessagne, F. & Schomerus, H. Selective enhancement of topologically induced interface states in a dielectric resonator chain. *Nat. Commun.* **6**, 6710 (2015).
72. Bahari, B. et al. Nonreciprocal lasing in topological cavities of arbitrary geometries. *Science* **358**, 636–640 (2017).
73. St-Jean, P. et al. Lasing in topological edge states of a one-dimensional lattice. *Nat. Photon.* **11**, 651–656 (2017).
74. Parto, M. et al. Edge-mode lasing in 1D topological active arrays. *Phys. Rev. Lett.* **120**, 113901 (2018).
75. Zhao, H. et al. Topological hybrid silicon microlasers. *Nat. Commun.* **9**, 981 (2018).
76. Harari, G. et al. Topological insulator laser: theory. *Science* **359**, eaar4003 (2018).
77. Bandres, M. A. et al. Topological insulator laser: experiments. *Science* **359**, eaar4005 (2018).
78. Dikopoltsev, A. et al. Topological insulator vertical-cavity laser array. *Science* **373**, 1514–1517 (2021).
79. Liu, Y. G., Jung, P. S., Parto, M., Christodoulides, D. N. & Khajavikhan, M. Gain-induced topological response via tailored long-range interactions. *Nat. Phys.* **17**, 704–709 (2021).
80. Yang, L., Li, G., Gao, X. & Lu, L. Topological-cavity surface-emitting laser. *Nat. Photon.* **16**, 279–283 (2022).
81. Schumer, A. et al. Topological modes in a laser cavity through exceptional state transfer. *Science* **375**, 884–888 (2022).
82. Hu, B. et al. Non-Hermitian topological whispering gallery. *Nature* **597**, 655–659 (2021).
83. Okuma, N., Kawabata, K., Shiozaki, K. & Sato, M. Topological origin of non-Hermitian skin effects. *Phys. Rev. Lett.* **124**, 086801 (2020).
84. Wojcik, C. C., Sun, X.-Q., Bzdušek, T. & Fan, S. Homotopy characterization of non-Hermitian Hamiltonians. *Phys. Rev. B* **101**, 205417 (2020).
85. Hu, H. & Zhao, E. Knots and non-Hermitian bloch bands. *Phys. Rev. Lett.* **126**, 010401 (2021).
86. Wang, K., Dutt, A., Wojcik, C. C. & Fan, S. Topological complex-energy braiding of non-Hermitian bands. *Nature* **598**, 59–64 (2021).
87. Kawabata, K., Bessho, T. & Sato, M. Classification of exceptional points and non-Hermitian topological semimetals. *Phys. Rev. Lett.* **123**, 066405 (2019).
88. Yao, S. & Wang, Z. Edge states and topological invariants of non-Hermitian systems. *Phys. Rev. Lett.* **121**, 086803 (2018).
89. Zhang, X., Zhang, T., Lu, M.-H. & Chen, Y.-F. A review on non-Hermitian skin effect. *Adv. Phys. X* **7**, 2109431 (2022).
90. Zhang, K., Yang, Z. & Fang, C. Universal non-Hermitian skin effect in two and higher dimensions. *Nat. Commun.* **13**, 2496 (2022).
91. Weidemann, S. et al. Topological funneling of light. *Science* **368**, 311–314 (2020).
Experimental demonstration of the non-Hermitian skin effect.
92. Gao, P., Willatzen, M. & Christensen, J. Anomalous topological edge states in non-Hermitian piezophononic media. *Phys. Rev. Lett.* **125**, 206402 (2020).
93. Zhang, L. et al. Acoustic non-Hermitian skin effect from twisted winding topology. *Nat. Commun.* **12**, 6297 (2021).
94. Li, Z. & Mong, R. S. Homotopical characterization of non-Hermitian band structures. *Phys. Rev. B* **103**, 155129 (2021).
95. Shen, H., Zhen, B. & Fu, L. Topological band theory for non-Hermitian Hamiltonians. *Phys. Rev. Lett.* **120**, 146402 (2018).
Topological band theory for non-Hermitian systems.
96. El-Ganainy, R. et al. Non-Hermitian physics and PT symmetry. *Nat. Phys.* **14**, 11–19 (2018).
97. Özdemir, Ş. K., Rotter, S., Nori, F. & Yang, L. Parity–time symmetry and exceptional points in photonics. *Nat. Mater.* **18**, 783–798 (2019).
98. Miri, M.-A. & Alù, A. Exceptional points in optics and photonics. *Science* **363**, eaar7709 (2019).
99. Zhou, H. et al. Observation of bulk Fermi arc and polarization half charge from paired exceptional points. *Science* **359**, 1009–1012 (2018).
100. Cerjan, A. et al. Experimental realization of a Weyl exceptional ring. *Nat. Photon.* **13**, 623–628 (2019).
101. Yang, Z. & Hu, J. Non-Hermitian Hopf-link exceptional line semimetals. *Phys. Rev. B* **99**, 081102 (2019).
102. Bergholtz, E. J., Budich, J. C. & Kunst, F. K. Exceptional topology of non-Hermitian systems. *Rev. Mod. Phys.* **93**, 015005 (2021).
103. Cui, X., Zhang, R.-Y., Chen, W.-J., Zhang, Z.-Q. & Chan, C. T. Symmetry-protected topological exceptional chains in non-Hermitian crystals. Preprint at https://arxiv.org/abs/2204.08052 (2022).
104. Ghorashi, S. A. A., Li, T., Sato, M. & Hughes, T. L. Non-Hermitian higher-order Dirac semimetals. *Phys. Rev. B* **104**, L161116 (2021).
105. Yang, X., Cao, Y. & Zhai, Y. Non-Hermitian Weyl semimetals: non-Hermitian skin effect and non-Bloch bulk–boundary correspondence. *Chin. Phys. B* **31**, 010308 (2022).
106. Weidemann, S., Kremer, M., Longhi, S. & Szameit, A. Topological triple phase transition in non-Hermitian Floquet quasicrystals. *Nature* **601**, 354–359 (2022).
107. Oppenheim, A. V. et al. *Signals & Systems* (Pearson Educación, 1997).
108. Boyd, R. W. *Nonlinear Optics* (Academic Press, 2020).
109. Smirnova, D., Leykam, D., Chong, Y. D. & Kivshar, Y. Nonlinear topological photonics. *Appl. Phys. Rev.* **7**, 021306 (2020).
110. Maczewsky, L. J. et al. Nonlinearity-induced photonic topological insulator. *Science* **370**, 701–704 (2020).
Experimental realization of nonlinear photonic topological insulators.
111. Chaunsali, R. & Theocharis, G. Self-induced topological transition in phononic crystals by nonlinearity management. *Phys. Rev. B* **100**, 014302 (2019).
112. Darabi, A. & Leamy, M. J. Tunable nonlinear topological insulator for acoustic waves. *Phys. Rev. Appl.* **12**, 044030 (2019).
113. Xia, S. et al. Nonlinear tuning of PT symmetry and non-Hermitian topological states. *Science* **372**, 72–76 (2021).
114. Mukherjee, S. & Rechtsman, M. C. Observation of Floquet solitons in a topological bandgap. *Science* **368**, 856–859 (2020).
115. Leykam, D. & Chong, Y. D. Edge solitons in nonlinear-photonic topological insulators. *Phys. Rev. Lett.* **117**, 143901 (2016).
116. Ivanov, S. K., Kartashov, Y. V., Szameit, A., Torner, L. & Konotop, V. V. Floquet edge multicolor solitons. *Laser Photon. Rev.* **16**, 2100398 (2022).
117. Zangeneh-Nejad, F. & Fleury, R. Nonlinear second-order topological insulators. *Phys. Rev. Lett.* **123**, 053902 (2019).
118. Kirsch, M. S. et al. Nonlinear second-order photonic topological insulators. *Nat. Phys.* **17**, 995–1000 (2021).
Observation of nonlinear second-order photonic topological insulators.
119. Yang, Y. et al. Synthesis and observation of non-Abelian gauge fields in real space. *Science* **365**, 1021–1025 (2019).
Experimental synthesis of non-Abelian gauge fields in real space.
120. Chen, Y. et al. Non-Abelian gauge field optics. *Nat. Commun.* **10**, 3125 (2019).
121. Nayak, C., Simon, S. H., Stern, A., Freedman, M. & Sarma, S. D. Non-Abelian anyons and topological quantum computation. *Rev. Mod. Phys.* **80**, 1083–1159 (2008).
122. Boross, P., Asbóth, J. K., Széchenyi, G., Oroszlány, L. & Pályi, A. Poor man's topological quantum gate based on the Su–Schrieffer–Heeger model. *Phys. Rev. B* **100**, 045414 (2019).
123. Neef, V. et al. Three-dimensional non-Abelian quantum holonomy. *Nat. Phys.* **13**, 30–34 (2023).
124. Chen, Z.-G., Zhang, R.-Y., Chan, C. T. & Ma, G. Classical non-Abelian braiding of acoustic modes. *Nat. Phys.* **18**, 179–184 (2022).
125. Sun, Y.-K. et al. Non-Abelian Thouless pumping in photonic waveguides. *Nat. Phys.* **18**, 1080–1085 (2022).
126. Brosco, V., Pilozzi, L., Fazio, R. & Conti, C. Non-Abelian Thouless pumping in a photonic lattice. *Phys. Rev. A* **103**, 063518 (2021).
127. You, O. et al. Observation of non-Abelian Thouless pump. *Phys. Rev. Lett.* **128**, 244302 (2022).
128. Fruchart, M., Zhou, Y. & Vitelli, V. Dualities and non-Abelian mechanics. *Nature* **577**, 636–640 (2020).
129. Patil, Y. S. et al. Measuring the knot of non-Hermitian degeneracies and non-commuting braids. *Nature* **607**, 271–275 (2022).
130. Zhang, Q. et al. Observation of acoustic non-Hermitian Bloch braids and associated topological phase transitions. *Phys. Rev. Lett.* **1307**, 017201 (2023).
131. Tang, W., Ding, K. & Ma, G. Experimental realization of non-Abelian permutations in a three-state non-Hermitian system. *Natl Sci. Rev.* **9**, nwac010 (2022).
132. Schnyder, A. P., Ryu, S., Furusaki, A. & Ludwig, A. W. Classification of topological insulators and superconductors in three spatial dimensions. *Phys. Rev. B* **78**, 195125 (2008).
133. Wu, Q., Soluyanov, A. A. & Bzdušek, T. Non-Abelian band topology in noninteracting metals. *Science* **365**, 1273–1277 (2019).
Theoretical framework of non-Abelian band topology.
134. Guo, Q. et al. Experimental observation of non-Abelian topological charges and edge states. *Nature* **594**, 195–200 (2021).
135. Ünal, F. N., Bouhon, A. & Slager, R.-J. Topological Euler class as a dynamical observable in optical lattices. *Phys. Rev. Lett.* **125**, 053601 (2020).
136. Tiwari, A. & Bzdušek, T. Non-Abelian topology of nodal-line rings in PT-symmetric systems. *Phys. Rev. B* **101**, 195130 (2020).
137. Ezawa, M. Topological Euler insulators and their electric circuit realization. *Phys. Rev. B* **103**, 205303 (2021).
138. Jiang, B. et al. Experimental observation of non-Abelian topological acoustic semimetals and their phase transitions. *Nat. Phys.* **17**, 1239–1246 (2021).
139. Peng, B., Bouhon, A., Monserrat, B. & Slager, R.-J. Phonons as a platform for non-Abelian braiding and its manifestation in layered silicates. *Nat. Commun.* **13**, 423 (2022).
140. Bzdušek, T., Wu, Q., Rüegg, A., Sigrist, M. & Soluyanov, A. A. Nodal-chain metals. *Nature* **538**, 75–78 (2016).
141. Wang, M. et al. Experimental observation of non-Abelian earring nodal links in phononic crystals. *Phys. Rev. Lett.* **128**, 246601 (2022).
142. Bouhon, A. et al. Non-Abelian reciprocal braiding of Weyl points and its manifestation in ZrTe. *Nat. Phys.* **16**, 1137–1143 (2020).
143. Jiang, T. et al. Four-band non-Abelian topological insulator and its experimental realization. *Nat. Commun.* **12**, 6471 (2021).
144. Mermin, N. D. The topological theory of defects in ordered media. *Rev. Mod. Phys.* **51**, 591–648 (1979).
145. Chaikin, P. M. & Lubensky, T. C. *Principles of Condensed Matter Physics* (Cambridge Univ. Press, 1995).
146. Yazyev, O. V. & Louie, S. G. Electronic transport in polycrystalline graphene. *Nat. Mater.* **9**, 806–809 (2010).
147. Machida, T. et al. Zero-energy vortex bound state in the superconducting topological surface state of Fe(Se,Te). *Nat. Mater.* **18**, 811–815 (2019).
148. Vozmediano, M. A., Katsnelson, M. & Guinea, F. Gauge fields in graphene. *Phys. Rep.* **496**, 109–148 (2010).

149. Teo, J. C. Y. & Kane, C. L. Topological defects and gapless modes in insulators and superconductors. *Phys. Rev. B* **82**, 115120 (2010).
150. Teo, J. C. Y. & Hughes, T. L. Existence of Majorana-fermion bound states on disclinations and the classification of topological crystalline superconductors in two dimensions. *Phys. Rev. Lett.* **111**, 047006 (2013).
151. Slager, R.-J., Mesaros, A., Juričić, V. & Zaanen, J. Interplay between electronic topology and crystal symmetry: dislocation-line modes in topological band insulators. *Phys. Rev. B* **90**, 241403 (2014).
152. Ran, Y., Zhang, Y. & Vishwanath, A. One-dimensional topologically protected modes in topological insulators with lattice dislocations. *Nat. Phys.* **5**, 298–303 (2009).
153. Read, N. & Green, D. Paired states of fermions in two dimensions with breaking of parity and time-reversal symmetries and the fractional quantum Hall effect. *Phys. Rev. B* **61**, 10267 (2000).
154. Jackiw, R. & Rossi, P. Zero modes of the vortex-fermion system. *Nucl. Phys. B* **190**, 681–691 (1981).
Theoretical framework for zero modes bound to a vortex.
155. Hou, C.-Y., Chamon, C. & Mudry, C. Electron fractionalization in two-dimensional graphene-like structures. *Phys. Rev. Lett.* **98**, 186809 (2007).
156. Ivanov, D. A. Non-Abelian statistics of half-quantum vortices in p-wave superconductors. *Phys. Rev. Lett.* **86**, 268–271 (2001).
157. Gao, P. & Christensen, J. Topological vortices for sound and light. *Nat. Nanotechnol.* **16**, 487–489 (2021).
158. Gao, P. et al. Majorana-like zero modes in kekulé distorted sonic lattices. *Phys. Rev. Lett.* **123**, 196601 (2019).
Experiment on an acoustic state bound to a topological vortex.
159. Gao, P. & Christensen, J. Topological sound pumping of zero-dimensional bound states. *Adv. Quantum Technol.* **3**, 2000065 (2020).
160. Chen, C.-W. et al. Mechanical analogue of a majorana bound state. *Adv. Mater.* **31**, 1904386 (2019).
161. Ma, J., Xi, X., Li, Y. & Sun, X. Nanomechanical topological insulators with an auxiliary orbital degree of freedom. *Nat. Nanotechnol.* **16**, 576–583 (2021).
162. Menssen, A. J., Guan, J., Felce, D., Booth, M. J. & Walmsley, I. A. Photonic topological mode bound to a vortex. *Phys. Rev. Lett.* **125**, 117401 (2020).
163. Gao, X. et al. Dirac-vortex topological cavities. *Nat. Nanotechnol.* **15**, 1012–1018 (2020).
164. Noh, J. et al. Braiding photonic topological zero modes. *Nat. Phys.* **16**, 989–993 (2020).
165. Sheng, C. et al. Bound vortex light in an emulated topological defect in photonic lattices. *Light. Sci. Appl.* **11**, 243 (2022).
166. Fu, L. Topological crystalline insulators. *Phys. Rev. Lett.* **106**, 106802 (2011).
167. Li, T., Zhu, P., Benalcazar, W. A. & Hughes, T. L. Fractional disclination charge in two-dimensional C_n-symmetric topological crystalline insulators. *Phys. Rev. B* **101**, 115115 (2020).
168. Peterson, C. W., Li, T., Jiang, W., Hughes, T. L. & Bahl, G. Trapped fractional charges at bulk defects in topological insulators. *Nature* **589**, 376–380 (2021).
169. Liu, Y. et al. Bulk–disclination correspondence in topological crystalline insulators. *Nature* **589**, 381–385 (2021).
170. Deng, Y. et al. Observation of degenerate zero-energy topological states at disclinations in an acoustic lattice. *Phys. Rev. Lett.* **128**, 174301 (2022).
171. Wang, Q., Xue, H., Zhang, B. & Chong, Y. D. Observation of protected photonic edge states induced by real-space topological lattice defects. *Phys. Rev. Lett.* **124**, 243602 (2020).
172. Xia, B., Zhang, J., Tong, L., Zheng, S. & Man, X. Topologically valley-polarized edge states in elastic phononic plates yielded by lattice defects. *Int. J. Solids Struct.* **239**, 111413 (2022).
173. Xue, H. et al. Observation of dislocation-induced topological modes in a three-dimensional acoustic topological insulator. *Phys. Rev. Lett.* **127**, 214301 (2021).
174. Ye, L. et al. Topological dislocation modes in three-dimensional acoustic topological insulators. *Nat. Commun.* **13**, 508 (2022).
175. Lustig, E. et al. Photonic topological insulator induced by a dislocation in three dimensions. *Nature* **609**, 931–935 (2022).
176. Zhang, Z. et al. Pseudospin induced topological corner state at intersecting sonic lattices. *Phys. Rev. B* **101**, 220102 (2020).
177. Biesenthal, T. et al. Fractal photonic topological insulators. *Science* **376**, 1114–1119 (2022).
178. Ortix, C. Electrons broken into pieces at crystal defects. *Nature* **589**, 356–357 (2021).
179. Zhao, H. et al. Non-Hermitian topological light steering. *Science* **365**, 1163–1166 (2019).

Acknowledgements X.Z. and M.-H.L. are supported by the National Natural Science Foundation of China (grant number 12222407) and the National Key R&D Program of China (grant numbers 2018YFA0306200 and 2021YFB3801800). J.C. acknowledges support from the Spanish Ministry of Science and Innovation through a Consolidación Investigadora grant (CNS2022-135706). J.C. also acknowledges discussions with P. San-Jose.

Author contributions All authors contributed equally.

Competing interests The authors declare no competing interests.

Additional information
Correspondence and requests for materials should be addressed to Ming-Hui Lu or Johan Christensen.
Peer review information *Nature* thanks Yidong Chong, Alexander Khanikaev and the other, anonymous, reviewer(s) for their contribution to the peer review of this work.
Reprints and permissions information is available at http://www.nature.com/reprints.
Publisher's note Springer Nature remains neutral with regard to jurisdictional claims in published maps and institutional affiliations.